

CrossMark
click for updatesCite this: *RSC Adv.*, 2016, 6, 29769

Catalytic transformation of glycerol to 1-propanol by combining zirconium phosphate and supported Ru catalysts†

Mengpan Wang,^a Hanmin Yang,^b Yinzheng Xie,^a Xiaohui Wu,^a Chen Chen,^a Wenbo Ma,^a Qifeng Dong^a and Zhenshan Hou^{*ac}

The one-pot hydrogenolysis of biomass-derived glycerol to 1-propanol has been investigated over sequential two-layer catalysts in a continuous-flow fixed-bed reactor. The zirconium phosphate layer was packed in the upper layer for dehydration of glycerol into acrolein and the supported Ru catalysts were in the second layer for the sequential hydrogenation of acrolein to 1-propanol. It was observed that the second layer catalyst with the strong acid sites would cause the formation of glycerol degradation products such as methanol, ethanol, methane and carbon dioxide etc., while 2%Ru/SiO₂ with weak acid sites afforded the highest selectivity for 1-propanol. The sequential packing of zirconium phosphate and the 2%Ru/SiO₂ catalytic system can give full glycerol conversions at 77% selectivity of 1-propanol, as well as exhibiting long-term stability (80 h). Carbonaceous deposits were a main reason for deactivation and the deactivated catalysts can be regenerated conveniently by calcinations in air. The present approach afforded an effective one-pot hydrogenolysis of glycerol to biopropanol, which could bring about the benign development of the biodiesel industry.

Received 29th January 2016

Accepted 14th March 2016

DOI: 10.1039/c6ra02682f

www.rsc.org/advances

1. Introduction

Fossil fuel consumption has been increasing greatly for the past decades due to human activity. It is considered as the main cause of the greenhouse effect. Thus scientists have begun looking for alternatives to fossil energy, such as renewable biomass resources.^{1–3} Glycerol is one of the top-12 building block chemicals identified by the U.S. Department of Energy.⁴ Glycerol is a by-product from biodiesel manufacture by transesterification of plant and animal oils with methanol, and this could replace the traditional commercial route starting from propylene.⁵ Recently, researchers had put much attention on transforming glycerol to value-added chemicals. According to the articles published in the past few years, glycerol can be catalytically converted into valuable fine chemicals by oxidation, hydrogenolysis, dehydration, pyrolysis, steam reforming, etherification, esterification, oligomerization and polymerization, etc.⁶ One of the most important reactions is selective

hydrogenolysis of glycerol to propanediols (PDOs).⁷ 1,2-Propanediol (1,2-PDO) is usually achieved by the selective hydrogenolysis of propylene oxide in petroleum engineering and which is often used in pharmaceutical industry, customer care products, antifreeze and tobacco industry.⁸ Alternatively, different metals including Cu, Ni, Ru, Pt loaded on C, SiO₂, γ -Al₂O₃, ZnO, ZrO₂ and Cr₂O₃ have been used for glycerol hydrogenolysis to 1,2-PDO.^{9–20} On the other hand, 1,3-propanediol (1,3-PDO) is also widely used as a monomer for synthesizing polymers and normally available commercially by hydration of acrolein,⁸ while the recent research demonstrated that WO₃, ZrO₂, AlPO₄ and ReO_x supporting Pt, Ir catalysts can afford 1,3-PDO selectively by hydrogenolysis of glycerol.^{21–29} However, few articles have studied on the direct conversion of glycerol to 1-propanol (1-PO) up to date, although 1-PO is a valuable chemicals used as solvent, organic intermediate and raw materials.^{30,31}

Recently, 1-PO could be obtained by a process that can convert glycerol-derived PDOs to 1-PO.^{32–34} For example, RhReO_x/SiO₂ (Re/Rh = 0.5) catalyst gave high yields of 1-PO (66%) by the hydrogenolysis of 1,2-PDO at 393 K and 8.0 MPa initial H₂ pressure.³² In addition, amorphous zirconia-supported niobium catalysts also exhibited selectivity favouring propanol (approximately 39%) at 85.0% conversion of 1,2-PDO at 290 °C under 1 atm N₂.³³ When 1,3-PDO was used as feed and hydrogenolyzed at 230 °C and 6 MPa H₂ pressure, 1-PO was found to be the main product over Ni/Al₂O₃ and Ni/SiO₂ catalysts.³⁴

Regarding the synthetic route above, the one-pot hydrogenolysis of glycerol to biopropanols would be more

^aKey Laboratory for Advanced Materials, Research Institute of Industrial Catalysis, East China University of Science and Technology, Shanghai 200237, China. E-mail: houzhenshan@ecust.edu.cn; Tel: +86 21 64251686

^bKey Laboratory of Catalysis and Materials Science of the State Ethnic Affairs Commission, Ministry of Education, South-Central University for Nationalities, Wuhan 430074, Hubei Province, China

^cDepartment of Chemical and Environmental Engineering, Xinjiang Institute of Engineering, Urumqi 830011, China

† Electronic supplementary information (ESI) available. See DOI: 10.1039/c6ra02682f

preferential when concerned sustainability and energy efficiency, in comparison with the processes based on petroleum-derived ethylene, propylene or glycerol-derived PDOs. It has been reported that Pd/C catalyst gave a promising 1-PO selectivity (85 mol%) under batch-wise conditions through direct hydrogenolysis of glycerol solutions, but the conversion of glycerol was very low (2 mol%).³⁵ The continuous-flow fixed-bed reactors are the preferred reactors for heterogeneous catalysis where the reactions take place on solid catalyst surfaces. Recently, the one-step production of long-chain hydrocarbons from waste-biomass-derived chemicals using bi-functional heterogeneous catalysts has been developed.³⁶ Furthermore, a sequential two-layer catalytic system containing H β zeolite and Ni/Al₂O₃ catalyst in a fixed-bed reactor has also been reported for the hydrogenolysis of glycerol into 1-PO in high selectivity (69%) at high glycerol conversions (about 100%).³⁷

In the previous studies, our group has indicated that zirconium phosphate (ZrP) catalyst was very efficient and selective for gas phase dehydration of glycerol to acrolein.³⁸ Although acrolein is an important intermediate for the further industrial production, it is highly toxic and hard to storage. In this work, we attempted to use a sequential packing of the ZrP and hydrogenation catalysts in a fixed-bed reactor for hydrogenolysis of glycerol. The ZrP catalyst layer was packed before the hydrogenation catalyst layer. Considering that Ru component is highly efficient for unsaturated C=C and C=O hydrogenation, the different supported Ru catalysts have been prepared and screened as the second layer for transforming acrolein produced by the first layer ZrP catalyst into 1-PO in a fixed-bed continuous flow reactor.

2. Experimental

2.1. Materials

Zirconium oxychloride, ammonium dihydrogen phosphate, glycerol, silver nitrate silicon dioxide, aluminum oxide, niobium pentoxide were purchased from Sino pharm Chemical Reagent Co. Ltd. (Shanghai, China). The all-Na type Na β zeolite with a Si/Al ratio of 200 and NaZSM-5 with a Si/Al ratio of 30 was bought from ShenTan Catalysts Company (Shanghai, China). Before use, the Na β zeolite and NaZSM-5 zeolite were exchanged with NH₄Cl (1 M) solution three times and washed without Cl⁻ by deionized water. Then the materials were dried at 110 °C overnight, followed by calcination in air at 450 °C for 4 h to get the H-type zeolite. High purity N₂ (99.999%) and H₂ (99.999%) was supplied by ShangNong Gas Factory. Distilled water used in this work was produced by our own laboratory. All other chemicals (analytical grade) were from Sino pharm Chemical Reagent Co. Ltd. And used as received without any further purification.

2.2. Catalyst preparation

The amorphous zirconium phosphates were prepared by a precipitation method according to the previous procedure.³⁹ Briefly, an aqueous solution of NH₄H₂PO₄ (1.0 mol L⁻¹, 64 mL) was added dropwise to an aqueous solution of ZrOCl₂·8H₂O

(1.0 mol L⁻¹, 32 mL) at a molar ratio of P/Zr = 2. The mixture was stirred over night at room temperature, then filtered, and washed with deionized water until the pH of the filtrate reached to 6 and no Cl⁻ was detected by an acidic AgNO₃ solution. The resulting material was dried for 12 h at 100 °C, followed by calcination at 400 °C for 4 h in a muffle furnace prior to reaction. The elemental analysis demonstrated that the actual molar ratio of phosphate to zirconia was 1.54.

The supported Ru catalysts including 2%Ru/SiO₂, 2%Ru/Al₂O₃, 2%Ru/Nb₂O₅, 2%Ru/H β and 2%Ru/HZSM-5 were prepared by incipient wetness method. As a typical example, 0.054 g RuCl₃·3H₂O was dissolved in 1 mL H₂O, and this solution was joined to 1.0 g SiO₂. Then the dispersion was stirring vigorously for 1 h, stewing 24 h and dried at 120 °C for 12 h. The resulting material was reduced *in situ* at 400 °C for 1 h prior to reaction or various characterizations and denoted as 2%Ru/SiO₂. The other reduced Ru catalysts such as 2%Ru/Al₂O₃, 2%Ru/Nb₂O₅, 2%Ru/H β and 2%Ru/HZSM-5 have also been prepared in a similar method.

2.3. Catalyst characterization

X-ray diffraction (XRD) analysis of the fresh and used catalysts were performed in the 2 θ range of 10–80° on an Rigaku D/MAX 2550 VB/PC instrument using a graphite crystal a monochromator. The textural properties from N₂ adsorption isotherms were obtained on Quanta chrome NOVA 2200e equipment. The surface area was obtained from the isotherms in the relative pressure range of 0.0–0.35. Pore volume was determined at *p/p*₀ of 0.99. The inductively coupled plasma-atomic emission spectroscopy (ICP-AES) analysis was performed on a Varian ICP-710ES instrument. The sample was first treated with a hydrofluoric acid and nitric acid solution, and then was heated to 60 °C in an oil bath to remove hydrofluoric acid, followed by dissolving with water. HRTEM was performed in a JEOL JEM 2010 transmission electron microscope operating at 200 kV with a nominal resolution of 0.25 nm. The samples for TEM were prepared by dropping the aqueous solutions containing the NPs onto the carbon-coated Cu grids. The Raman spectra were obtained with an Invia-Reflex Raman spectrometer using a 514.5 nm excitation source. The IR spectrum of the pyridine-adsorbed catalyst was obtained in the transmission mode using a Nicolet Model 710 spectrometer. First, the catalyst (25 mg) was ground into fine powder and pressed into a very thin self-supporting wafer. The disc was mounted in a quartz IR cell equipped with a CaF₂ window. Then, the sample was subjected to a standard pre-treatment involving heat treatment at 300 °C in vacuum for 4 h. All the adsorption studies were carried out at 20 °C. Pyridine was adsorbed at the partial pressure at 20 °C under vacuum. The spectra of pyridine bonded by Brønsted and Lewis acid sites were recorded. The amount of acid sites of the different catalysts was obtained with temperature-programmed desorption of ammonia (NH₃-TPD). About 100 mg of catalyst was loaded in a quartz tube. Prior to each test, the sample was pre-treated in He at 300 °C for 1 h, cooled to 50 °C to remove surface water. Then, the sample was maintain at 50 °C for 1 h and saturated with a 10% NH₃-in-N₂ mixture, and then

flushed by He for 1 h to remove physically adsorbed ammonia. Then, the sample was heated to 800 °C at a heating rate of 10 °C min⁻¹ in the same flow of He. The profiles of desorption were recorded using a thermal conductivity detector (TCD), which was calibrated by a pulse-gas with known amount of NH₃. Thermal analysis of the catalysts was conducted on a Netzsch STA 449C thermal analyzer. The sample was placed in an Al₂O₃ crucible and heated in flowing air (30 mL min⁻¹) from 50 to 800 °C at a rate of 10 °C min⁻¹. The sample was dried overnight at 100 °C prior to the measurement.

2.4. Catalytic reaction

The hydrogenation of glycerol was carried out in a vertical fixed-bed stainless-steel reactor (1.1 cm i.d., length 60 cm). The ZrP catalyst was tableted and then crushed and sieved to 20–40 mesh particles for the catalytic reaction tests. The supported Ru catalysts were also sieved to 20–40 mesh particles. These two catalysts were packed in this fixed-bed reactor to be two layers, with the ZrP catalyst was set at the upper layer and the supported Ru catalysts at the second layer. The quartz wool was filled between two catalyst layers. A constant weight (1 g) of each catalyst layer was sandwiched in the middle of the reactor with quartz wool and quartz sand for supporting the catalyst and evaporation of the reactants. The temperature was controlled by a thermocouple placed in the middle of the catalyst bed. Prior to the reaction, catalyst was reduced at 400 °C for 1 h with 10% H₂-in-N₂ (0.1 MPa, 30 mL min⁻¹) and surface passivating treatment under N₂. After the temperature of reactor was constant, the feedstock, an aqueous solution containing 10 wt% glycerol, was then pumped into the reactor (0.04 mL min⁻¹) and driven through the catalyst bed by hydrogen flow. The reaction product were condensed in a cryogenic cooling system and collected every two hours for offline analysis using a GC 112A gas chromatograph equipped with an FFAP capillary column (30 m long, 0.32 mm i.d., 0.33 μm film thickness) and an Agilent 6890/5973 GC-MS System equipped with a HP-5MS column (30 m long, 0.25 mm i.d., 0.25 μm film thickness) and flame ionization detector (FID). Volatile compounds that were not retained in the cold trap were absorbed in ethanol and also analyzed by offline GC. The gaseous products were collected by a gas bag and analyzed by offline GC with thermal conductivity detector (TCD). For quantitative measurements, *n*-butanol was used as the internal standard. The conversion of glycerol and yield towards products were calculated as follows:

$$\text{Conversion(\%)} = \frac{\text{amount of glycerol converted(mole)}}{\text{total amount of glycerol in the feed(mole)}} \times 100\%$$

$$\text{Selectivity(\%)} = \frac{\text{amount of a product(mole)}}{\text{amount of glycerol converted(mole)}} \times \frac{\text{number of carbon atoms in the product}}{3} \times 100\%$$

Carbon yield in liquid products(%)

$$= \frac{\text{carbon atoms found in the liquid products(mole)}}{\text{carbon atoms of glycerol converted(mole)}} \times 100\%$$

3. Results and discussion

3.1. Catalyst characterization

From the literature reports, it is evident that glycerol hydrogenolysis involves several consecutive as well as parallel reactions and the product profile strongly depends upon the catalyst, promoters and reaction conditions. In this work, ZrP catalyst was adopted for the dehydration of glycerol to acrolein on the first layer. Thus ZrP catalyst was first characterized in details. TG pattern of ZrP was shown from 50 °C to 800 °C (Fig. 1(a)). It showed a fast weight loss from 50 °C to 200 °C due to the continuous dehydration of ZrP catalyst, and then the platform from 200 °C to 450 °C indicated that the ZrP catalysts has a good thermal stability. Actually, it has also been reported that the porous structure of ZrP has remarkable thermal stability even after calcination at 800 °C, which could allow it to be used in high-temperature reaction.⁴⁰ In addition, as shown in Fig. 1(b), the XRD patterns of the ZrP showed two broad peaks in the ranges of 10–40° and 40–70° respectively, indicating its amorphous nature.³⁹ The amorphous zirconium phosphate has a high surface area (101.3 m² g⁻¹) after calcination at 400 °C for 4 h (Table 1), and it had similar BET surface areas to that reported by Kamiya *et al.*³⁹ The N₂ adsorption-desorption isotherm is a type IV isotherm (Fig. S1†). The zirconium phosphate catalyst exhibits a uptake of nitrogen at low relative pressures (*p/p*₀) of 0.1–0.4, indicating that the pore sizes are mainly present in the ranges of micropore. BJH analysis of the pore size distribution on the adsorption isotherm reveals a pore size distribution centred around 1.7 nm (Fig. S2†).

The acidic properties of calcined ZrP samples were investigated by temperature-programmed desorption of ammonia analysis and infrared spectroscopy of adsorbed pyridine, and the results were shown in Fig. 1(c) and (d), respectively. The sample showed a little desorption of ammonia in the temperature range of 50–200 °C, indicating the presence of little numbers of weak acid sites (Fig. 1(c)). However, it was clear that the amounts of the medium strength acid sites (desorption in the temperature range of 200–350 °C) were much more than that of the strong acid sites (desorption in the temperature range of (>350 °C)) (Table 1). Total acidity (calculated from total area under the peaks in Fig. 1(c)) for ZrP was 1.03 mmol g⁻¹ (Table 1), which was close to that of previous report.⁴¹

In the next step, the type of acidic site on ZrP catalysts was determined by infrared spectroscopy of adsorbed pyridine and the spectra in the range of 2000–1200 cm⁻¹ are shown in Fig. 1(d). There are mainly three bands in this region. Pyridine adsorbed FT-IR spectra of the ZrP materials show sharp bands at 1543 cm⁻¹, which are the characteristic bands of the typical pyridinium ion (PyH⁺) confirming the presence of Brønsted acid sites. This Brønsted acidity within the catalysts could be due to

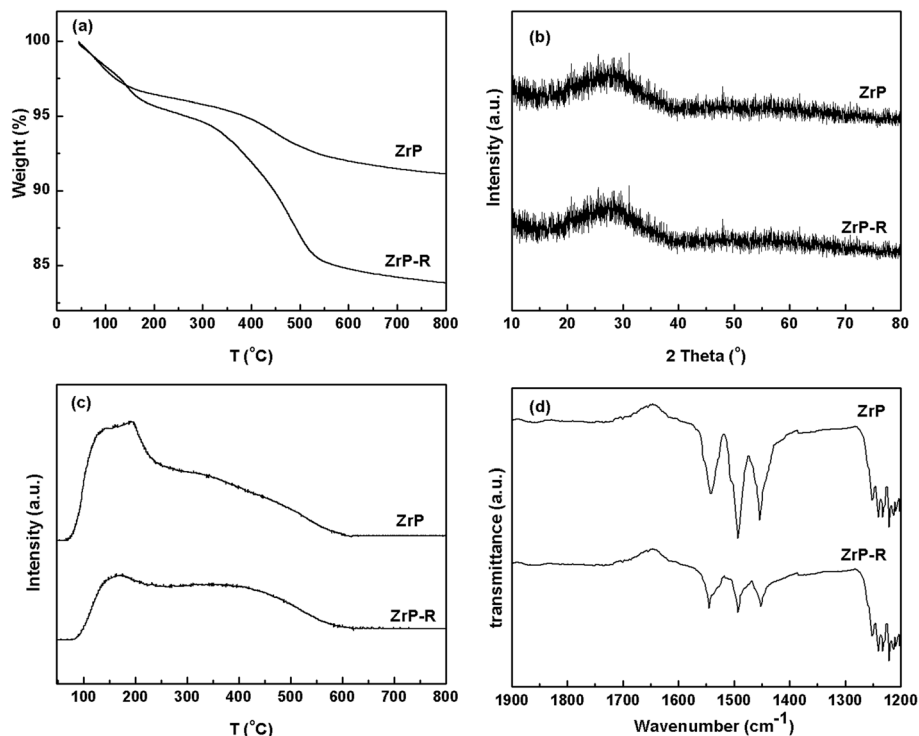


Fig. 1 The characterization of ZrP and ZrP-R catalysts (a) TG curves; (b) XRD patterns; (c) NH_3 -TPD profiles; (d) pyridine-adsorbed FT-IR spectra.

Table 1 Physicochemical properties of ZrP catalysts

| Catalysts | Surface area ($\text{m}^2 \text{g}^{-1}$) | Pore size (nm) | Pore volume ($\text{cm}^3 \text{g}^{-1}$) | NH_3 desorbed before 350 °C ($\text{mmol NH}_3 \text{g}^{-1}$) | NH_3 desorbed after 350 °C ($\text{mmol NH}_3 \text{g}^{-1}$) | Total acidity ($\text{mmol NH}_3 \text{g}^{-1}$) |
|-----------|---|----------------|---|---|--|--|
| ZrP | 101.3 | 1.7 | 0.22 | 0.85 | 0.18 | 1.03 |
| ZrP-R | 75.8 | 1.2 | 0.14 | 0.63 | 0.04 | 0.67 |

the presence of a reasonable amount of P(OH) groups in the ZrP. Further, the band at 1492 cm^{-1} , which could be attributed to the adsorption of pyridine in Brønsted and Lewis sites is also present in ZrP samples at the same time. The band at about 1453 cm^{-1} , corresponding to the adsorbed pyridine at the Lewis acid site (PyL) is clearly observed.^{42,43}

In this work, the Ru-supported catalysts were functioned as hydrogenation and normally packed in the layer after the ZrP catalyst. Fig. 2 showed the XRD patterns of all supports and these supported Ru catalysts. The presence Fig. 2(a) of one broad peaks in the ranges of $10\text{--}30^\circ$ indicated that SiO_2 owns amorphous nature.⁴⁴ The (020), (121), (420), (110) and (424) planes are corresponding to the typical pattern of the Al_2O_3 (Fig. 2(b)) (JCPDS 46-1131).⁴⁵ The (001), (180), (201), (331), (381) and (382) planes are corresponding to the typical pattern of the Nb_2O_5 (Fig. 2(c)) (JCPDS 27-1003).⁴⁶ The Fig. 2(d) shows the characteristic signals of the parent H β catalyst at 2Theta angles of $7\text{--}8^\circ$ and $21\text{--}22^\circ$ (JCPDS 45-0406).⁴⁷ The Fig. 2(d) shows the characteristic signals of the parent HZSM-5 catalyst at 2Theta angles of $7\text{--}10^\circ$ and $23\text{--}25^\circ$ (JCPDS 42-0024).⁴⁸ Additionally, compared to the standard XRD pattern of metal state Ru (JCPDS

65-7646), no obvious Ru(0) characteristic diffraction peaks of (100), (002), (101) (102), (110) and (103) planes over all supported Ru catalysts were observed in Fig. 2(a–e), which was ascribed to the low contents of metals or the high dispersion of the metal particles.

The textural and surface properties of the samples are shown in Table 2, where acid density was derived from the profile of NH_3 -TPD (Fig. 3) and the mean size of Ru particles from the TEM images (Fig. 4). Obviously, the supports with higher surface area could be favourable for forming smaller Ru particles (Table 2, entries 1–5). In addition, 2%Ru/ SiO_2 catalyst has the maximum amount of weak and medium strong acid site (0.85 mmol g^{-1}), but has the minimal total amount acid sites among all catalysts due to the absence of strong acid site (Table 2, entries 1–5). In contrast, the HZSM-5 catalyst has the maximum amounts of the strong acid site (1.04 mmol g^{-1}) and total acid sites (1.7 mmol g^{-1}). It can be seen clearly that the amounts of the strong acid sites (desorption after the temperature of 350 °C) decreased in the order: 2%Ru/HZSM-5 > 2%Ru/ Nb_2O_5 > 2%Ru/ Al_2O_3 > 2%Ru/H β > 2%Ru/ SiO_2 .

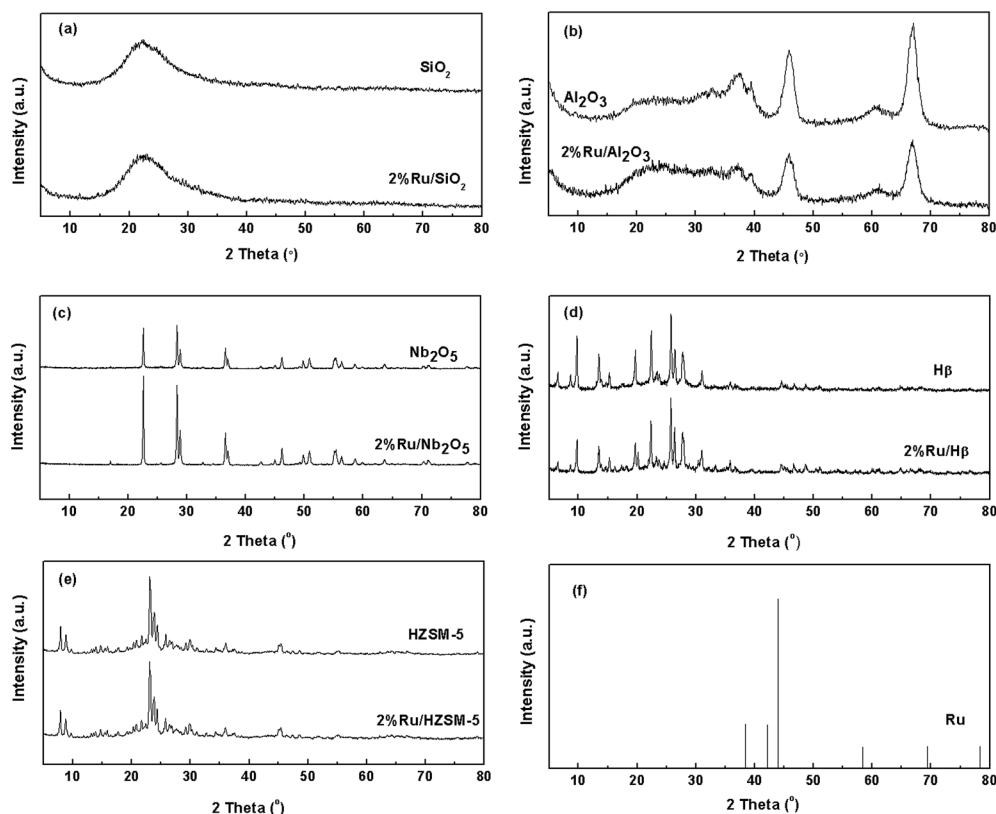


Fig. 2 XRD patterns of (a) SiO₂ and 2%Ru/SiO₂ reduced at 400 °C under N₂/H₂; (b) Al₂O₃ and 2%Ru/Al₂O₃ reduced at 400 °C under N₂/H₂; (c) Nb₂O₅ and 2%Ru/Nb₂O₅ reduced at 400 °C under N₂/H₂; (d) Hβ and 2%Ru/Hβ reduced at 400 °C under N₂/H₂; (e) HZSM-5 and 2%Ru/HZSM-5 reduced at 400 °C under N₂/H₂. (f) Standard metal state Ru (JCPDS 65-1863).

Table 2 Physicochemical properties of different supported Ru catalysts

| Entries | Catalysts | Surface area (m ² g ⁻¹) | Pore size (nm) | Pore volume (cm ³ g ⁻¹) | Ru size (nm) | NH ₃ desorbed before 350 °C (mmol NH ₃ g ⁻¹) | NH ₃ desorbed after 350 °C (mmol NH ₃ g ⁻¹) | Total acidity (mmol NH ₃ g ⁻¹) |
|---------|-------------------------------------|--|----------------|--|--------------|--|---|---|
| 1 | 2%Ru/SiO ₂ | 258.6 | 10.7 | 0.69 | 2.8 | 0.85 | 0.01 | 0.86 |
| 2 | 2%Ru/Al ₂ O ₃ | 165.2 | 9.4 | 0.37 | 5.0 | 0.66 | 0.37 | 1.03 |
| 3 | 2%Ru/Nb ₂ O ₅ | 99.0 | 5.6 | 0.13 | 12.0 | 0.65 | 0.64 | 1.29 |
| 4 | 2%Ru/Hβ | 302.3 | 2.3 | 0.18 | 5.5 | 0.71 | 0.28 | 0.99 |
| 5 | 2%Ru/HZSM-5 | 298.8 | 2.3 | 0.17 | 3.0 | 0.66 | 1.04 | 1.70 |
| 6 | 2%Ru/SiO ₂ -R | 175.6 | 1.2 | 0.14 | 4.1 | 0.43 | 0.00 | 0.43 |

3.2. Catalytic activity

We first examined the activity of the first ZrP layer catalyst for the dehydration of glycerol to acrolein before performing glycerol hydrogenolysis over a sequential two-layer catalyst system. It was observed that ZrP catalyst afforded 82% selectivity to acrolein with the full conversion of glycerol, and no obvious deactivation over 50 h under N₂ flow (30 mL min⁻¹), indicating that ZrP was a highly hydrothermal stable and water-tolerant solid acid catalyst.³⁸ Surface acidic sites played an important role in improving the activity, selectivity to acrolein, and life of catalysts. It should be noting that the result is almost the same if the N₂ was replaced by H₂ (Table 3, entries 1 and 2). The selectivity of acrolein was as much as 81.2%, implying the gas

(H₂ or N₂) did not have obvious effect on dehydration of glycerol to acrolein over the ZrP catalyst. What's more, when the hydrogen pressure increased above 2.0 MPa, it also did not have an obvious impact on the selectivity of acrolein (Table 3, entry 3). The characterization from pyridine-adsorbed FT-IR spectra indicated that there existed both Lewis acidic sites and Brønsted ones on the surface of calcined ZrP catalyst (Fig. 1(d)). It is well known that in catalytic reactions, in which excess of water is present at a relatively high temperature (285–330 °C), at least some Lewis acidic sites are converted to Brønsted ones.⁴⁹ From the previous investigation, it was known that Brønsted acid sites with medium and high strength were active sites for acrolein production from glycerol dehydration while Lewis acid

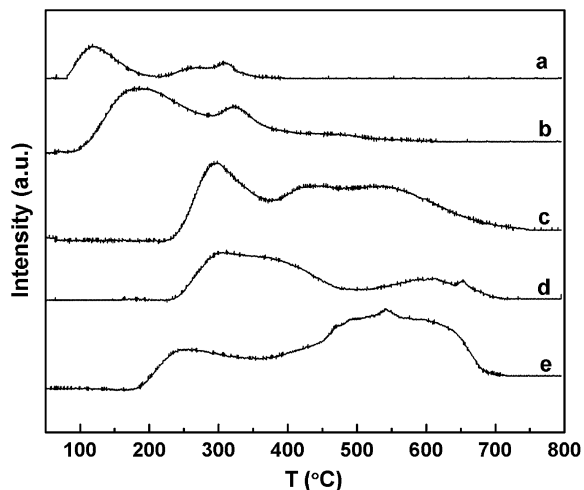


Fig. 3 NH_3 -TPD profiles of different catalysts. (a) 2%Ru/SiO₂; (b) 2%Ru/Al₂O₃; (c) 2%Ru/Nb₂O₅; (d) 2%Ru/H β ; (e) 2%Ru/HZSM-5.

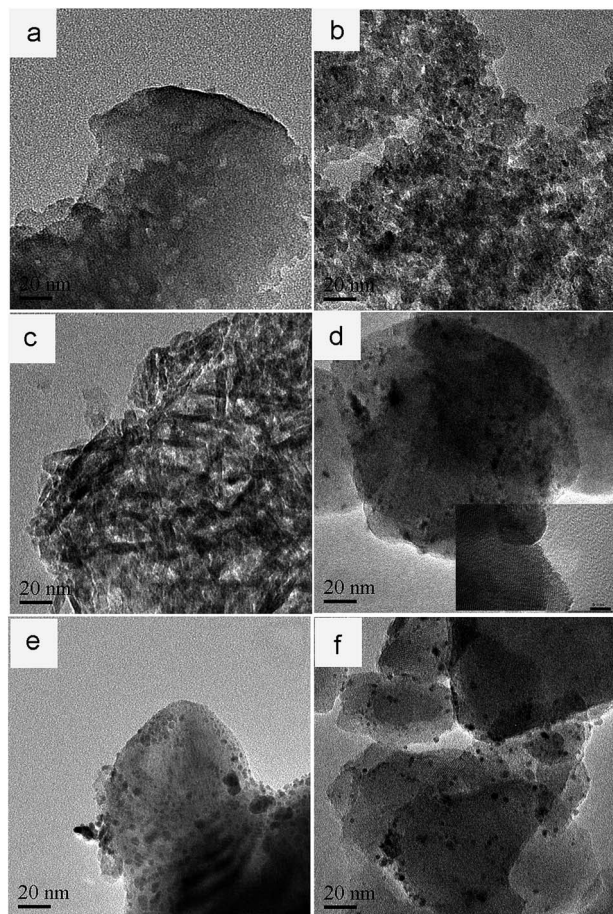


Fig. 4 TEM images of the different catalysts. (a) 2%Ru/SiO₂ reduced at 400 °C under N₂/H₂; (b) 2%Ru/SiO₂-R after 100 h on stream; (c) 2%Ru/Al₂O₃ reduced at 400 °C under N₂/H₂; (d) 2%Ru/Nb₂O₅ reduced at 400 °C under N₂/H₂ (inset represents the image of HRTEM, scale bar is 5 nm); (e) 2%Ru/H β reduced at 400 °C under N₂/H₂; (f) 2%Ru/HZSM-5 reduced at 400 °C under N₂/H₂.

sites were responsible for the formation of acetol and other by-products.⁵⁰ This implied that the ZrP catalyst with the large amounts of medium strength Brønsted acid sites were beneficial for improving the selectivity toward acrolein.³⁸

Next, the gas phase hydrogenolysis of glycerol was carried out over the present two-layer catalysts. As shown in Table 3, entries 4–8, the main products included 1-PO and 1,2-PDO and acrolein, while acetol, ethanol, and methanol were detected as minor side products in liquid phase. Other small amount of gaseous products such as CO₂, CO and CH₄, which possibly resulted from the decomposition of cleavage of C–C bonds, can be also detected by GC with TCD. Despite these gaseous products, the carbon yield in liquid phase was always over 80% except that 2%Ru/HZM-5 used as the second layer catalyst gave only 44.6% carbon yield (Table 3, entry 4). The further GC analysis proved that the tail gas contained a large amount of CO₂, CO and CH₄.

According to the characterization results of catalysts as shown in Table 2, we can see that 2%Ru/SiO₂, 2%Ru/Al₂O₃, 2%Ru/H β and 2%Ru/HSM-5 have a relatively high BET surface area while 2%Ru/Nb₂O₅ have a low BET surface area, which resulted in the larger Ru particles (about 12 nm) on Nb₂O₅, as compared with that of others. The larger Ru particles could show low hydrogenation ability for acrolein,⁵¹ leading to high selectivity to acrolein (38.4%) in the products (Table 3, entry 5). In contrast, those catalysts with small Ru particles showed very low selectivity to acrolein. For example, the second layer catalysts like 2%Ru/Al₂O₃, 2%Ru/H β which have a close Ru particles size and acid properties give 66.3% and 66.2% of selectivities to 1-PO, respectively (Table 3, entry 6 and 7). Nevertheless, the second layer Ru/HZSM-5 catalyst afforded relatively high selectivity to methanol and ethanol and also the carbon yield in liquid phase is very poor because a large amount of gases was formed likely due to the presence of a large amount of strong acid sites (Table 2, entry 4), resulting in the cleavage of carbon–carbon bond and thus the very high selectivities to gaseous products, methanol and ethanol. The present results is similar with that of previous research,⁵² which indicated that the acidity of HZSM-5 has a significant effect on the activity of Ru catalysts and products electivity in the hydrogenolysis of glycerol.

It should be noticing that the single-layer 2%Ru/SiO₂ catalyst only gave moderate selectivity to 1,2-PDO (48.0%) with poor glycerol conversion (18%) (Table 3, entry 9). The main by-products were ethanol (in 9.7% selectivity) and methanol (in 4.2% selectivity). Acetol, CO₂, CO and CH₄ were also observed as minor products, and the selectivity of 1-PO is only 2.5%. When 1.0 g of ZrP was packed in the layer before the 1.0 g of 2%Ru/SiO₂ layer, both of the glycerol conversion and selectivity to 1-PO were improved significantly (Table 3, entry 8). On the other hand, the selectivity to 1,2-PDO was dramatically decreased from 48% to 7.5%. In addition, when 10% acrolein aqueous solution was employed as a feed and converted only by Ru/SiO₂ catalyst. It was found that the acrolein conversion was more than 99% and the selectivity to 1-PO reached to 96% (Table 3, entry 11). This result demonstrates that for the two-layer catalysts, acrolein produced from glycerol dehydration over the first layer catalyst (ZrP) could be hydrogenated into 1-PO effectively

Table 3 Catalytic performances of the hydrogenolysis of glycerol using different catalysts^a

| Entries | Catalysts | | Con. % | Sel. % | | | | | | | Carbon yield in liquid products % |
|---------|------------------|-------------------------------------|--------|-------------------|----------------------|----------|--------|---------|----------|---------------------|-----------------------------------|
| | The first layer | The second layer | | 1-PO ^b | 1,2-PDO ^c | Acrolein | Acetol | Ethanol | Methanol | Others ^d | |
| 1 | ZrP ^e | None | 100 | 0.0 | 0.0 | 82.0 | 10.3 | 0.0 | 0.0 | 7.7 | 92.3 |
| 2 | ZrP ^f | None | 100 | 0.0 | 0.0 | 81.7 | 10.8 | 0.0 | 0.0 | 7.6 | 92.5 |
| 3 | ZrP | None | 100 | 0.0 | 0.0 | 81.3 | 11.5 | 0.0 | 0.0 | 7.2 | 92.8 |
| 4 | ZrP | 2%Ru/HZSM-5 | 100 | 13.2 | 2.6 | 2.3 | 1.4 | 16.2 | 8.9 | 55.4 | 44.6 |
| 5 | ZrP | 2%Ru/Nb ₂ O ₅ | 100 | 29.7 | 8.5 | 38.4 | 6.8 | 2.2 | 1.7 | 12.7 | 87.4 |
| 6 | ZrP | 2%Ru/H β | 100 | 66.3 | 4.3 | 2.6 | 3.1 | 3.9 | 3.4 | 16.4 | 83.5 |
| 7 | ZrP | 2%Ru/Al ₂ O ₃ | 100 | 66.2 | 5.9 | 5.4 | 2.9 | 1.7 | 1.0 | 16.9 | 83.1 |
| 8 | ZrP | 2%Ru/SiO ₂ | 100 | 76.5 | 7.5 | 1.6 | 1.2 | 0.7 | 0.6 | 11.9 | 88.0 |
| 9 | None | 2%Ru/SiO ₂ | 18.1 | 2.5 | 48.0 | 0.0 | 4.2 | 9.7 | 4.2 | 33.9 | 67.0 |
| 10 | None | 2%Ru/SiO ₂ ^g | 42.0 | 57.4 | — | 0.0 | 0.0 | 5.8 | 6.5 | 30.3 | 65.1 |
| 11 | None | 2%Ru/SiO ₂ ^h | 99.5 | 96 | — | — | — | 1.4 | 2.2 | 0.4 | 98.2 |

^a Hydrolysis of glycerol using ZrP catalyst (1.0 g) as the first layer, and the supported Ru catalysts (1.0 g) as the second layer in a fixed-bed reactor. Temperature: 315 °C; H₂ pressure: 2 MPa; flow rate of glycerol aqueous solution (10% wt): 0.04 mL min⁻¹; flow rate of H₂ = 30 mL min⁻¹. ^b 1-Propanol. ^c 1,2-Propanediol. ^d Others gas and condensation products. ^e N₂ (0.1 MPa). ^f H₂ (0.1 MPa). ^g 10% 1,2-PDO aqueous solution as a feed. ^h 10% acrolein aqueous solution as a feed.

by the sequential Ru/SiO₂ catalyst (Table 3, entries 3, 8 and 11). The addition of the ZrP catalyst directed the hydrodeoxygenation of glycerol toward a higher degree, and thus improved the selectivity to 1-PO.

Since the ZrP, coupling with 2%Ru/SiO₂ catalyst exhibited promising catalytic performance, the following investigations were conducted on the two layer catalysts. The influence of temperature on glycerol hydrogenolysis was illustrated in Fig. 5(a), in which showed that glycerol conversion improved from 95% (285 °C) to 100% (300 °C). While, the selectivity to 1-PO increased remarkably to a maximum at 315 °C and then decreased. It can be seen that both acrolein and acetol co-existed in low selectivity due to the high hydrogenation activity over 2%Ru/SiO₂ catalyst. Meantime, the main by-product 1,2-PDO which is hydrogenised from acetol is decreased when the temperature increased from 285 °C to 315 °C, indicating that 1,2-PDO would undergo a dehydration and sequential hydrogenation at higher temperature over Ru/SiO₂

catalyst (Fig. 5(a)). This can be further evidenced by the fact that when 1,2-PDO was used as a feed and hydrogenated by a single layer 2%Ru/SiO₂ catalyst, the conversion of 1,2-PDO is 42.0% and the selectivity to 1-PO reached up to 57.4% (Table 3, entry 10). Moreover, as reaction temperature increasing on ZrP catalyst, the selectivity of acrolein increased, accompanying with that of acetol decreased,³⁷ which thus resulted in a decline of the selectivity of 1,2-PDO derived from acetol hydrogenation over 2%Ru/Al₂O₃ catalyst accordingly (Fig. 5(a)). On the other hand, the selectivity of acrolein is always below 2.5%, and this meant that the second layer 2%Ru/SiO₂ catalyst exhibited promising hydrogenation performance even the temperature is below 315 °C. Whereas the decrease of selectivity to 1-PO at higher temperature (>315 °C) is related to the formation of large amounts of undesired by-products, such as the over hydrogenolysis product propane, and the degradation products methanol, ethanol, methane, carbon dioxide. This is in agreement with the results reported by Esti van Ryneveld *et al.*³⁴

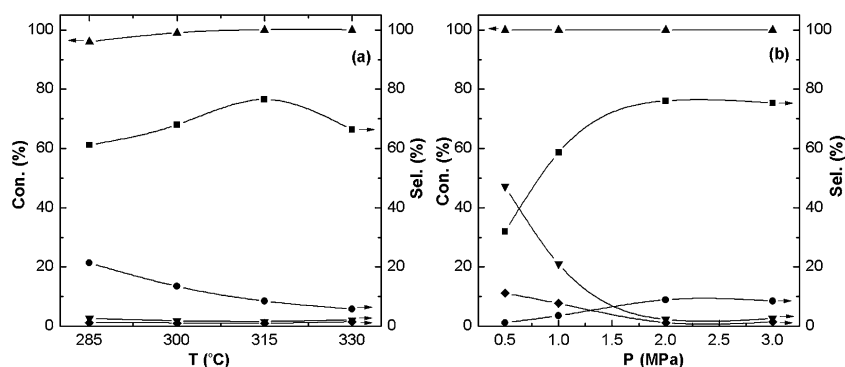
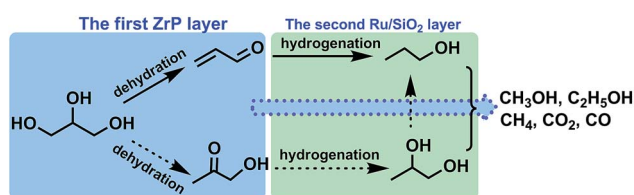


Fig. 5 (a) Effect of reaction temperature and (b) hydrogen pressure on glycerol hydrogenolysis over the two layer catalysts. (▲) glycerol, (■) 1-propanol, (●) 1,2-propanediol, (▼) acrolein, (◆) acetol. Reaction conditions: (a) pressure = 2 MPa; flow rate of glycerol solution (10% wt) = 0.04 mL min⁻¹; flow rate of H₂ = 30 mL min⁻¹. (b) Temperature = 315 °C; flow rate of glycerol solution (10% wt) = 0.04 mL min⁻¹; flow rate of H₂ = 30 mL min⁻¹.

Fig. 5(b) shows the effect of hydrogen pressure on the catalytic performance of glycerol hydrogenolysis over two layer catalysts at 315 °C. The selectivity of 1-PO enhanced from 32.0% to 76.5% while the selectivity of acrolein decreased sharply from 47.2% to 2.3% as the hydrogen pressure was increased from 0.5 MPa to 2 MPa, revealing that although the increase of the hydrogen pressure does not affect the product distribution on the first ZrP layer (Table 3, entries 2 and 3), the hydrogenation rate of the second layer 2%Ru/SiO₂ catalyst increased greatly. This implied that the 2%Ru/SiO₂ catalyst was highly active for acrolein hydrogenation to 1-PO, even at a relatively low hydrogen pressure compared to previous report.³⁰ Additionally, as H₂ pressure increased to 2 MPa, the selectivity of 1,2-PDO increased slightly from 1.5% to 8.0% while the selectivity to acetol decreased from 11.8% to 2.2%, indicating that 1,2-PDO mainly resulted from the acetol hydrogenation. However, at least the portion of 1,2-PDO was also converted into 1-PO by dehydration and sequential hydrogenation route as discussed above. The further increasing hydrogen pressure above 2.0 MPa did not have an obvious impact on the selectivity of 1-PO Fig. 5(b).

Following on from our finding and previous report,³⁷ the possible reaction route involved in glycerol hydrogenolysis is proposed in Scheme 1. The acid-catalyzed dehydration of glycerol over the first ZrP catalyst layer initially formed acrolein as a main product and acetol as minor by-product, which can subsequently hydrogenate into 1-PO and 1,2-PDO over supported Ru catalysts, respectively. The intermediate such as 1,2-PDO can also undergo a dehydration and sequential hydrogenation route on the supported Ru catalyst to give 1-PO. Meantime, both of dehydration of glycerol and subsequent hydrogenation process would generate minor gas by-products including CO₂, CO and methane due to C-C bond cleavage.

The long-term performance of glycerol hydrogenolysis over two layer catalysts was conducted at 315 °C and 2.0 MPa, and the results are shown in Fig. 6. The catalytic activity did not decline obviously within 80 h under the present reaction conditions. Meanwhile, the product distribution did not show any appreciable change during the whole test. This result demonstrated that the two layer catalytic system was rather durable under hydrothermal conditions for glycerol hydrogenolysis and could be suitable for practical applications. The superior long-term performance of ZrP and 2%Ru/SiO₂ was mainly not only attributed to the large amount of middle strong acid sites on ZrP catalyst which can convert glycerol to acrolein, and also the highly active Ru sites dispersed on SiO₂ which can convert acrolein to 1-PO rapidly. As shown in



Scheme 1 Formation of the products from hydrogenolysis of glycerol.

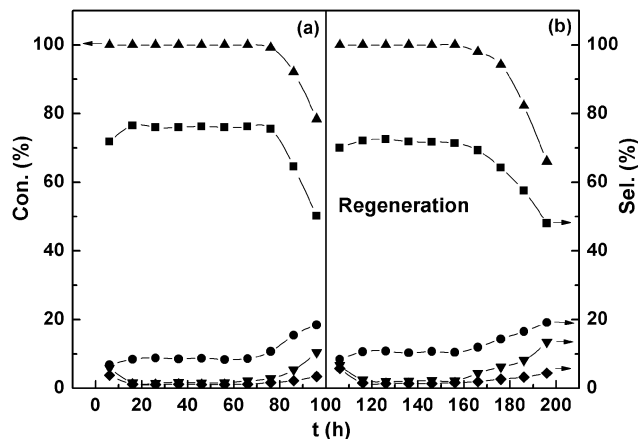


Fig. 6 Long-term performance of glycerol hydrogenolysis over ZrP and 2%Ru/SiO₂ catalysts. (a) The hydrogenolysis of glycerol was carried out for 100 h on stream; (b) after the catalyst was reacted for 100 h on stream, it was regenerated by calcining at 500 °C for 4 h and then continued on reaction for another 100 h. (▲) glycerol, (■) 1-propanol, (●) 1,2-propanediol, (▼) acrolein, (◆) acetol; reaction conditions: temperature = 315 °C; flow rate of glycerol solution (10% wt) = 0.04 mL min⁻¹; flow rate of H₂ = 30 mL min⁻¹. Pressure = 2 MPa.

Fig. 6, the conversion and selectivity to 1-PO reached to 100% and 77%, respectively, and both of them can keep stable as long as 80 h although they decreased over 80 h on stream. However, when the catalyst was regenerated by calcining at 500 °C for 4 h after reaction for 100 h, it can be reused for another 100 h in continuous flow process. The conversion of glycerol still achieved a high level, although the selectivity to 1-PO (around 72%) decreased slightly.

It was observed that the ZrP catalyst after reaction for 100 h showed a slight dark colour, indicating the possible presence of a considerable amount of carbonaceous deposits on the surface of catalyst. From profiles of TG of catalysts in air as shown Fig. 1(a) and 7, we can see that both the spent ZrP catalyst (ZrP-R) and the spent 2%Ru/SiO₂ catalysts (2%Ru/SiO₂-R) are all have an obvious weight loss due to coking removal around 500 °C, as compared to the fresh one. The rise of the weight below 300 °C could be attributed to the oxidation of Ru(0). This indicated that the carbon deposition can be removed simply by calcinations in air, which allowed regenerating catalyst and thus making a longer performance of the catalyst.

Sequentially, the various carbon deposits of the spent catalysts were analysed by Raman spectroscopy and the results are shown in Fig. 8. All spectra showed two major peaks at about 1346 cm⁻¹ and 1573 cm⁻¹. The peak at 1573 cm⁻¹ represented graphitic, designated as G-band and the peak at 1346 cm⁻¹ was attributed to defects present in the structural units of graphite designated as D-band. This meant that the type of coke species on different catalysts was almost same.

The carbonaceous deposits pointed to a deactivation mechanism due to carbonaceous deposits blocking the catalytically active sites. The BET surface area of ZrP-R decreased to 75.8 m² g⁻¹, as compared with the fresh one (101.3 m² g⁻¹) (Table 1). In addition, the acid amounts of catalysts also decreased from 1.03

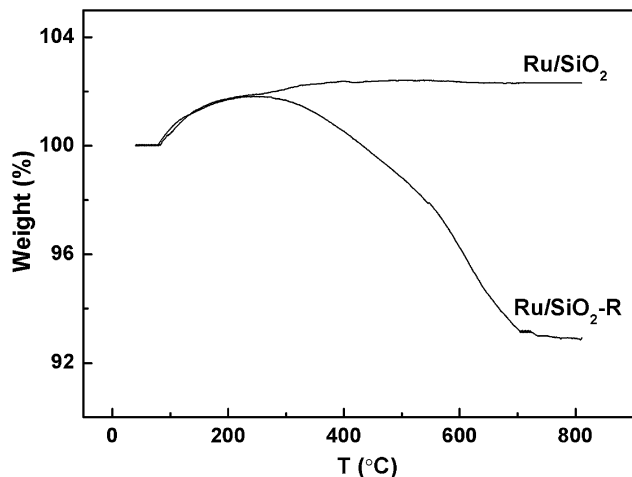


Fig. 7 TG curves of 2%Ru/SiO₂ and 2%Ru/SiO₂-R catalysts.

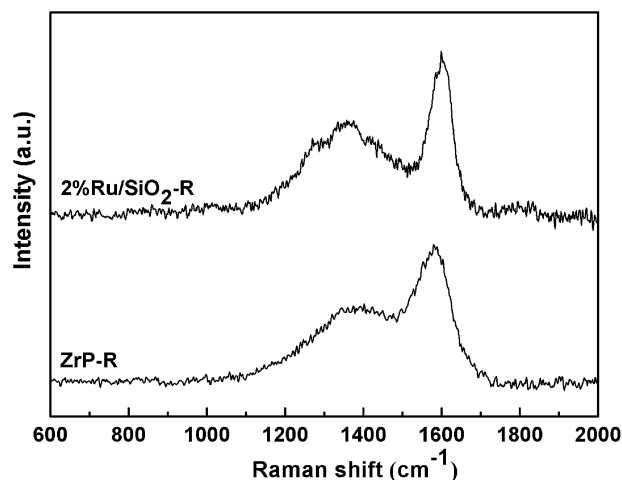


Fig. 8 The Raman spectra of the recovered catalysts after 100 h on stream.

mmol NH₃ g⁻¹ to 0.67 mmol NH₃ g⁻¹ (Table 1). What's more, the medium strength acid sites have decreased dramatically compared with the fresh catalyst, which led to the decrease of the selectivity of acrolein. Thus, selectivity of the 1-PO was decreased in a small degree. Meantime, the BET surface area of 2%Ru/SiO₂-R decreased from 258.6 m² g⁻¹ to 175.6 m² g⁻¹ and the acid amount of 2%Ru/SiO₂-R catalyst also decreased from 0.86 mmol NH₃ g⁻¹ to 0.43 mmol NH₃ g⁻¹. It should be noticing that the sizes of Ru particle on SiO₂ increased from 2.8 nm to 4.1 nm after 100 h on stream from TEM images (Table 2, entries 1 and 6). This might be the reason why the regenerated catalyst afforded slightly lower selectivity to 1-PO, but higher selectivity to acrolein, in comparison with the fresh one in the first run (Fig. 6).

4. Conclusion

In summary, the hydrogenolysis of glycerol solutions was performed by using a sequential two-layer catalytic system in

a fixed-bed reactor. It was found that the two sequential ZrP and Ru/SiO₂ layer catalyst system showed a superior selectivity (77%) to 1-propanol at full of glycerol conversion by a dehydration-hydrogenation route, where ZrP converted glycerol into acrolein while Ru/SiO₂ catalyst acrolein into 1-PO. The catalytic performance of glycerol hydrogenolysis depended on reaction temperature, hydrogen pressure. The present two layer catalyst exhibited an 80 h long-term performance and then can be regenerated for another 100 h by calcining on air to remove carbonaceous deposits. The strategy to develop an effective and green process in the present work might provide guidance for the sustainable production of valuable chemicals from biomass derived polyols.

Acknowledgements

The authors are grateful for support from the National Natural Science Foundation of China (21373082), innovation Program of Shanghai Municipal Education Commission (15ZZ031) and the Fundamental Research Funds for the Central Universities.

Notes and references

- 1 D. M. Alonso, S. G. Wettstein and J. A. Dumesic, *Chem. Soc. Rev.*, 2012, **41**, 8075–8098.
- 2 C. H. Zhou, X. Xia, C. X. Lin, D. S. Tong and J. Beltramini, *Chem. Soc. Rev.*, 2011, **40**, 5588–5617.
- 3 A. M. Ruppert, K. Weinberg and R. Palkovits, *Angew. Chem., Int. Ed.*, 2012, **51**, 2564–2601.
- 4 J. J. Bozell and G. R. Petersen, *Green Chem.*, 2010, **12**, 539.
- 5 G. W. Huber, S. Iborra and A. Corma, *Chem. Rev.*, 2006, **106**, 4044–4098.
- 6 C. H. Zhou, H. Zhao, D. S. Tong, L. M. Wu and W. H. Yu, *Catal. Rev.*, 2013, **55**, 369–453.
- 7 Y. Wang, J. Zhou and X. Guo, *RSC Adv.*, 2015, **5**, 74611–74628.
- 8 Y. Nakagawa and K. Tomishige, *Catal. Sci. Technol.*, 2011, **1**, 179.
- 9 S. Sato, M. Akiyama, R. Takahashi, T. Hara, K. Inui and M. Yokota, *Appl. Catal., A*, 2008, **347**, 186–191.
- 10 S. Xia, L. Zheng, L. Wang, P. Chen and Z. Hou, *RSC Adv.*, 2013, **3**, 16569.
- 11 A. Bienholz, H. Hofmann and P. Claus, *Appl. Catal., A*, 2011, **391**, 153–157.
- 12 Y. Feng, H. Yin, A. Wang, L. Shen, L. Yu and T. Jiang, *Chem. Eng. J.*, 2011, **168**, 403–412.
- 13 S. Xia, R. Nie, X. Lu, L. Wang, P. Chen and Z. Hou, *J. Catal.*, 2012, **296**, 1–11.
- 14 M. Checa, A. Marinas, J. M. Marinas and F. J. Urbano, *Appl. Catal., A*, 2015, **507**, 34–43.
- 15 M. Balarajua, V. Rekhua, B. L. A. Prabhavathi Devib, R. B. N. Prasadb, P. S. Sai Prasada and N. Lingaiah, *Appl. Catal., A*, 2010, **384**, 107–114.
- 16 D. Roy, B. Subramaniam and R. V. Chaudhari, *Catal. Today*, 2010, **156**, 31–37.
- 17 S.-H. Lee and D. J. Moon, *Catal. Today*, 2011, **174**, 10–16.
- 18 T. Miyazawa, Y. Kusunoki, K. Kunimori and K. Tomishige, *J. Catal.*, 2006, **240**, 213–221.

- 19 R. Rodrigues, N. Isoda, M. Gonçalves, F. C. A. Figueiredo, D. Mandelli and W. A. Carvalho, *Chem. Eng. J.*, 2012, **198**, 457–467.
- 20 S. N. Delgado, L. Vivier and C. Especel, *Catal. Commun.*, 2014, **43**, 107–111.
- 21 C. Deng, X. Duan, J. Zhou, D. Chen, X. Zhou and W. Yuan, *Catal. Today*, 2014, **234**, 208–214.
- 22 S. S. Priya, V. P. Kumar, M. L. Kantam, S. K. Bhargava and K. V. R. Chary, *RSC Adv.*, 2014, **4**, 51893–51903.
- 23 T. Kurosaka, H. Maruyama, I. Naribayashi and Y. Sasaki, *Catal. Commun.*, 2008, **9**, 1360–1363.
- 24 O. M. Daniel, A. DeLaRiva, E. L. Kunkes, A. K. Datye, J. A. Dumesic and R. J. Davis, *ChemCatChem*, 2010, **2**, 1107–1114.
- 25 L. Gong, Y. Lu, Y. Ding, R. Lin, J. Li, W. Dong, T. Wang and W. Chen, *Appl. Catal., A*, 2010, **390**, 119–126.
- 26 J. Oh, S. Dash and H. Lee, *Green Chem.*, 2011, **13**, 2004.
- 27 R. Arundhathi, T. Mizugaki, T. Mitsudome, K. Jitsukawa and K. Kaneda, *ChemSusChem*, 2013, **6**, 1345–1347.
- 28 Y. Nakagawa, Y. Shinmi, S. Koso and K. Tomishige, *J. Catal.*, 2010, **272**, 191–194.
- 29 Y. Nakagawa, X. Ning, Y. Amada and K. Tomishige, *Appl. Catal., A*, 2012, **433**, 128–134.
- 30 S. Zhu, Y. Zhu, S. Hao, H. Zheng, T. Mo and Y. Li, *Green Chem.*, 2012, **14**, 2607.
- 31 L. Yu, J. Yuan, Q. Zhang, Y.-M. Liu, H.-Y. He, K.-N. Fan and Y. Cao, *ChemSusChem*, 2014, **7**, 743–747.
- 32 Y. Amada, S. Koso, Y. Nakagawa and K. Tomishige, *ChemSusChem*, 2010, **3**, 728–736.
- 33 G. Peng, X. Wang, X. Chen, Y. Jiang and X. Mu, *J. Ind. Eng. Chem.*, 2014, **20**, 2641–2645.
- 34 E. van Ryneveld, A. S. Mahomed, P. S. van Heerden, M. J. Green, C. Holzapfel and H. B. Friedrich, *Catal. Sci. Technol.*, 2014, **4**, 832.
- 35 E. Ryneveld, A. S. Mahomed, P. S. Heerden and H. B. Friedrich, *Catal. Lett.*, 2011, **141**, 958–967.
- 36 C. Wen, E. Barrow and J. Hattrick-Simpers, *Phys. Chem. Chem. Phys.*, 2014, **16**, 3047–3054.
- 37 X. Lin, Y. Lv, Y. Xi, Y. Qu, D. L. Phillips and C. Liu, *Energy Fuels*, 2014, **28**, 3345–3351.
- 38 H. Gan, X. Zhao, B. Song, L. Guo, R. Zhang, C. Chen, J. Chen, W. Zhu and Z. Hou, *Chin. J. Catal.*, 2014, **35**, 1148–1156.
- 39 Y. Kamiya, S. Sakata, Y. Yoshinaga, R. Ohnishi and T. Okuhara, *Catal. Lett.*, 2004, **94**, 45–47.
- 40 A. Sinhamahapatra, N. Sutradhar, B. Roy, A. Tarafdar, H. C. Bajaj and A. B. Panda, *Appl. Catal., A*, 2010, **385**, 22–30.
- 41 Y. Liao, Q. Liu, T. Wang, J. Long, L. Ma and Q. Zhang, *Green Chem.*, 2014, **16**, 3305–3312.
- 42 S. K. Das, M. K. Bhunia, A. K. Sinha and A. Bhaumik, *ACS Catal.*, 2011, **5**, 493–501.
- 43 A. Corma, *Chem. Rev.*, 1995, **95**, 559–614.
- 44 E. S. Vasiliadou, E. Heracleous, I. A. Vasalos and A. A. Lemonidou, *Appl. Catal., B*, 2009, **92**, 90–99.
- 45 L. Ma, D. He and Z. Li, *Catal. Commun.*, 2008, **9**, 2489–2495.
- 46 I. Nowak and M. Ziolk, *Chem. Rev.*, 1999, **99**, 3603–3624.
- 47 S. Gomez, C. L. Marchena, M. S. Renzini, L. Pizzio and L. Pierella, *Appl. Catal., B*, 2015, **162**, 167–173.
- 48 Y. T. Kim, K.-D. Jung and E. D. Park, *Microporous Mesoporous Mater.*, 2010, **131**, 28–36.
- 49 R. Weingarten, G. A. Tompsett, W. C. Conner and G. W. Huber, *J. Catal.*, 2011, **279**, 174–182.
- 50 Y. Gu, S. Liu, C. Li and Q. Cui, *J. Catal.*, 2013, **301**, 93–102.
- 51 K. Chary, C. Srikanth and V. Venkatrao, *Catal. Commun.*, 2009, **10**, 459–463.
- 52 Y. Li, L. Ma, H. Liu and D. He, *Appl. Catal., A*, 2014, **469**, 45–51.